DMD Fast Forward. Published on September 22, 2011 as doi:10.1124/dmd.111.041806

TITLE PAGE

Inhibition of Human Liver Aldehyde Oxidase:

Implications for Potential Drug-drug Interactions

John T. Barr and Jeffrey P. Jones

Department of Chemistry, Washington State University, Pullman, WA, 99164

RUNNING TITLE PAGE

Running Title: Inhibition of Human Liver Aldehyde Oxidase: Implications for Potential Drug-drug Interactions

To whom correspondence should be addressed: Jeffrey P. Jones. Tel: 509-335-5983, Fax: 509-335-8867, Email: jpj@wsu.edu .

Text Pages (including references): 24

Tables: 2

Figures: 4

References: 25

Abstract : 192

Introduction : 746

Discussion : 1400

Abbreviations: DDI: Drug-drug interaction; AOX: aldehyde oxidase; HLC: human liver cytosol; DMSO: dimethyl sulfoxide; DCPIP: 2,6-dichlorophenolindophenol; LB: Lineweaver-Burk; IS: internal standard; 6-CQ: 6-chloroquinazolinone; E-S: enzyme-substrate.

DMD Fast Forward. Published on September 22, 2011 as DOI: 10.1124/dmd.111.041806
This article has not been copyedited and formatted. The final version may differ from this version.

ABSTRACT

During the course of our research efforts to understand the kinetics of human AOX as a xenobiotic clearing enzyme, we investigated the effect of 8 different inhibitors on the oxidation of the probe substrate phthalazine. Saturation kinetic parameters for phthalazine oxidation in human liver cytosol were found to be the following: K_m = 8.0 ± 0.4 μM and V_{max} = 4.3 ± 0.1 nmol/min/mg protein. Inhibitory potency of the inhibitors tested ranged from 0.1 μM to 5 μM. Of the 8 different inhibitor compounds tested, 7 were observed to inhibit through a mixed mode and 1 through a strictly competitive mode. A ratio of the K_{ii} and K_{is} values was used to assess the relative competitiveness of each inhibitor. For the mixed inhibitors, the mode of inhibition varied from mostly uncompetitive to predominantly competitive (K_{ii} / K_{is} values ranging from 0.1 to 15). The implications for potential drug-drug interactions and inhibition mechanism are discussed. We found two inhibitors, clozapine and chlorpromazine, that have a moderate predicted risk of drug-drug interactions based on the K_i value relative to inhibitor concentration in human plasma, having a calculated [I]/K_i value of 0.4 and 0.8 respectively.

INTRODUCTION

Knowledge of drug-drug interactions (DDIs) is of great importance in the process of drug development. Without prior knowledge of potential DDIs, a drug can fail in clinical trials or after final approval leading to higher costs of pharmaceuticals and the lack of potentially life-saving therapeutics. DDIs can be divided into two major categories. The first, the pharmacodynamic effect, occurs when the presence of one drug alters the response of a second administered drug through either an additive or antagonistic effect. The second, pharmacokinetic effect, occurs when one drug (the "precipitant" drug) affects the absorption, distribution, metabolism or excretion of a second drug (the "object" drug). Numerous examples of both classes of interactions have been shown to cause adverse effects in patients; however, the instances involving the pharmacokinetic effect are much more common.

Because various cytochrome p450 isoforms are responsible for phase I metabolism of approximately 80% of drugs on the market (Ortiz de Montellano, 2005), the drug interactions ascribed to clearance by these enzymes remain to be the major focus of clinical practice. However, the potential for drug interactions for the remaining 20% of drugs that are metabolized via pathways other than CYPs still exist. Little is known about the pharmacokinetic interactions of these other xenobiotic clearing enzymes such as the one of current focus: aldehyde oxidase.

Aldehyde oxidase (AOX) is a member of a group of molybdoflavo-enzymes that includes the more extensively studied xanthine oxidase. AOX has been found to play a role in the metabolism of many drugs and xenobiotic compounds. As its name implies, AOX is known for its ability to oxidize aldehydes to carboxylic acids. However, AOX is also involved in the oxidation of nitrogen containing heterocyclic compounds, as well as iminium ion intermediates (Brandaenge and Lindblom, 1979; Whittlesea and Gorrod, 1993).

In a recent review, the authors predicted a growing importance of aldehyde oxidase in drug metabolism (Pryde et al., 2010). This is primarily due to the recent growth in the number of aromatic azaheterocycle

moieties that are found in drug leads. These groups are typically installed in lead compounds for reasons including increased metabolic stability to cytochrome P450 oxidation (Chiba et al., 2001; Peng et al., 2010) and to enhance desired pharmacodynamic properties.

Unlike cytochrome P450 (Bibi, 2008), the potential drug interactions in human AOX has not been well characterized. To date only one pharmacokinetic drug interaction due to the inhibition of AOX, between cimetidine and zaleplon, has been discovered (Lake et al., 2002). Predicting drug interactions with AOX is also relatively more difficult than in cytochrome P450. This is primarily because animal models are poor predictors of human AOX activity due to the marked interspecies variation of expression levels and number of isoforms (Garattini and Terao, 2011). In recent study, researchers have made steps to further the understanding of the inhibition of human AOX and the implications on drug interactions (Obach, 2004; Obach et al., 2004).

In 2004, Obach et al. screened a library of 239 drugs and xenobiotics for potential inhibition of AOX (Obach et al., 2004). Of these 239 compounds, 36 inhibited oxidase activity by 80% or greater at a test concentration of 50 μM. The inhibitory potency of these 36 compounds was measured using an IC_{50} determination assay. A number of different classes of drugs exhibited potent inhibition of AOX. Of particular note, was the most potent inhibitor of all compounds that were tested, raloxifene, which has an IC_{50} value of approximately 3 nM.

A subsequent study by Obach focused on the mode and mechanism by which AOX was inhibited by raloxifene (Obach, 2004). For oxidation reactions studied, Obach found that the mode of inhibition was strictly uncompetitive. From this finding, the author concluded that there was a low risk of drug-drug interaction by raloxifene through an AOX mediated pathway.

In the present study, 8 different compounds of widely differing chemical structure were chosen to investigate the mode of inhibition of AOX (Figure 1). Of these 8, 6 were previously shown to have relatively high inhibition potency through an IC_{50} value determination assay. Our primary goal was to

elucidate the mode of inhibition for a number of potent inhibitors with varied chemical structure in order to provide insight into the potential for drug interactions, as well as provide information regarding the mechanism for inhibition. Secondarily, we wanted to compare the previously measured IC_{50} values of inhibitors to K_i values, in order to assess the overall effectiveness of an IC_{50} screening assay for predicting potential drug interactions.

METHODS

Chemicals Used and Enzyme Source

Phthalazine, 1-phthalazinone, 2-Methyl-4(3H)-quinazolinone, estradiol, ethinyl estradiol, chlorpromazine, clozapine, menadione, domperidone, and 2,6-dichlorophenolindophenol were purchased from Sigma-Aldrich (St. Louis, Mo). 6-chloroquinazolinone was synthesized in our lab using methods previously described (Alfaro et al., 2009). Human liver cytosol (HLC), pooled from 10 individual donors, was purchased from BD Biosciences (Woburn, MA).

Incubation Conditions

Incubations were performed using a modified technique as previously described by Obach and coworkers (Obach et al., 2004). Incubation mixtures consisted of phthalazine (with a final concentration ranging from 1.6 to 100 μM) and inhibitor of varying concentration in 25 mM potassium phosphate buffer, pH 7.4, containing 0.1 mM EDTA. Inhibitor stock solutions were made up in dimethyl sulfoxide (DMSO), and added to the incubation such that the total concentration of DMSO was exactly 1% (v/v). To the incubations without inhibitor, 1% neat DMSO was added. Previous experiments demonstrated that this concentration of DMSO had no effect on phthalazine oxidase activity (Obach et al., 2004).

The reaction was initiated at 37˚C in a shaking water bath incubator by addition of preincubated HLC at a final concentration of 0.05 mg total protein/mL in the reaction mixture. The final volume of reaction solution was 800 μL. Reaction vials were shaken in open air for 2.5 minutes. Upon which, the reactions were quenched with 200 μL of 1M formic acid, containing a known concentration of 2-methyl-4(3H)-quinazolinone as internal standard. Quenched samples were centrifuged for 10 minutes at 5,000 rpm using an Eppendorf centrifuge 5415 D, and the supernatant was collected for analysis.

HPLC-MS Assay

Samples were analyzed using an Agilent Technologies 1100 series high performance liquid chromatography system and an API4000 MS/MS system manufactured by Applied Biosystems/MDS Sciex. Chromatography was performed on a Synergi Polar Reverse Phase column (30 X 3.0 mm; 4 um; Phenomenex , Inc. , Torrance, CA).

Mobile phase A was comprised of 0.05% Formic acid and 0.2% Acetic Acid in water, and mobile phase B consisted of 90% CH3CN, 9.9% water, and 0.1% formic acid. The column was equilibrated at initial conditions of 95% mobile phase A for 0.3 min. Chromatographic separation was achieved using a linear gradient over the next 2.2 min to 25% mobile phase A. Mobile phase A was then held at 25% over 0.5 min, followed by a linear gradient back to 95% A over 0.5 min. The column was reequilibrated to initial conditions over the next 1.5 min. Total chromatographic assay time was 5 min per sample. The retention times for internal standard and metabolite was 2.5 and 2.8 min, respectively. An example chromatogram for internal standard and metabolite is shown in Supplemental Figure 1.

The optimized mass spectrometer tune parameters for 1-phthalazinone were as follows: collision gas, 8; curtain gas, 15; ion source gas 1, 4; ion source gas 2, 1; ionspray voltage, 3500; desolvation temperature 300; declustering potential, 50; entrance potential, 3; collision energy,30; collision cell exit potential, 10.

The analyte (1-phthalazinone) and internal standard (2-Methyl-4(3H)-quinazolinone) were detected using multiple reaction monitoring mode by monitoring the m/z transition from 161 to 120 and 147 to 118 respectively. The MS system was operated in positive ion mode. Quantitation of product was achieved by extrapolating from a standard curve ranging from 0 to 3.2 μM metabolite.

Experimental Duplication and Controls

Two controls were run with each batch of samples. The first control included omission of cytosol from the reaction and the second included the omission of phthalazine (substrate).

All K_i determinations were measured in duplicate for each inhibitor using different batches of pooled HLC. In the first K_i measurement, a total of 6 inhibitor concentrations (including no inhibitor) and 6 substrate concentrations (1.6, 3.1, 6.3, 25, 50, and 100 μM) were used. In the second (duplicate) K_i measurement done on a different day, a total of 4 concentrations of inhibitor (including no inhibitor) and 4 concentrations of substrate (1.6, 6.3, 50, 100 μM) were used. Fewer concentrations for inhibitor and substrate were analyzed for duplicate assays in order to expedite data collection and conserve resources and instrument usage.

Each individual reaction vial was measured by LCMS in triplicate and the average value was used for all calculations and plots.

Data analysis

Lineweaver-Burk plots and the subsequent replots of both y-intercept vs inhibitor concentration and slope vs. inhibitor concentration were made to visualize the kinetic data (Cook and Cleland, 2007) using Graphpad Prism version 4.03. Mode of inhibition was determined by visual inspection of Lineweaver-Burk plots and statistical analysis of slope and y-intercept replot data. The slopes of replot linear regression lines were analyzed using an F-test feature that is built in to the Graphpad Prism software. The F-test generates a p value that is used to determine statistical significance. A p value of 0.05 or less was used as the threshold value for whether or not the slope for each linear regression line of the replots were significantly nonzero. Graphs with significantly nonzero slopes in the regression line of the replot data for both slope and y-intercept were determined to be mixed mode type inhibition. Graphs with a significant nonzero slope in the regression line of the slope replot but not in the y-intercept replot were determined to be strictly competitive. Conversely, graphs with a significant nonzero slope in the regression line of the y-intercept replot but not in the slope replot were determined to be uncompetitive inhibition.

Once the mode of inhibition was selected, the data was fit to the appropriate non-linear regression model. Equations used for each model are shown below.

DMD Fast Forward. Published on September 22, 2011 as DOI: 10.1124/dmd.111.041806
This article has not been copyedited and formatted. The final version may differ from this version.

Competitive Inhibition Model: $v=Vapp[S]Kapp1+IKis+[S]$

Mixed Competitive Inhibition Model: $v= Vapp[S]Kapp1+IKis+S1+IKii$

Where v is the reaction velocity, V_{app} is the apparent V_{max}, [S] is the substrate concentration, K_{app} is the apparent Michaelis-Menten constant, [I] is the concentration of inhibitor, K_{is} is the dissociation constant for Enzyme-Inhibitor complex, and K_{ii} is the dissociation constant for Enzyme-Substrate-Inhibitor complex.

RESULTS

The AOX substrate chosen for this study was the aromatic azaheterocycle compound phthalazine. The oxidation reaction monitored in kinetic assays is shown in Figure 2. Phthalazine has been shown previously to be a substrate with a relatively high reaction rate and a high specificity for AOX (Panoutsopoulos and Beedham, 2004). Additionally, both phthalazine and its metabolite are commercially available compounds so quantitation of metabolite and substrate availability were not an issue.

Multiple concentrations of phthalazine (substrate) and inhibitor were incubated in the presence of pooled HLC from 10 individual donors. After a period of 2.5 minutes, the reaction was terminated with a formic acid solution containing a known concentration of internal standard, 2-methyl-4(3H)-quinazolinone. Kinetic data was measured using a liquid chromatography tandem mass spectrometry assay that monitored the formation of metabolite (1-phthalazinone). Figure 3 shows the substrate saturation curve for phthalazine oxidation. Saturation kinetic parameters were determined by non-linear regression analysis using the Michaelis–Menten kinetic model as follows: $K_m = 8.0 \pm 0.4$ μM and $V_{max} = 4.3 \pm 0.1$ nmol/min/mg protein.

We then determined the mode of inhibition by visual inspection of Lineweaver-Burk (LB) plots as well as analysis of the statistical significance in both slope and intercept replots. The details of statistical analysis can be found in the methods section of this text. The LB plots and replots for all 8 inhibitors are shown in Figure 4, and the LB plots for duplicate measurements can be found in the supplemental data in Supplemental Figure 2. All K_i values were determined by non-linear regression analysis using a global fit to the appropriate kinetic model.

Of the 8 compounds tested, 7 showed a mixed-mode type of inhibition, exhibiting some character of both uncompetitive and competitive inhibition. Table 1 provides a full account of the K_{is} and K_{ii} values obtained for the tested compounds. K_{is} is a measure of the affinity the inhibitor has for the free enzyme,

DMD Fast Forward. Published on September 22, 2011 as DOI: 10.1124/dmd.111.041806
This article has not been copyedited and formatted. The final version may differ from this version.

whereas K_{ii} is the affinity the inhibitor has for enzyme-substrate complex. In addition, a K_{ii}/K_{is} value was calculated for each compound as a metric of the degree of inhibition competitiveness. A larger K_{ii}/K_{is} value indicates a mode of inhibition that is relatively more competitive whereas a lower K_{ii}/K_{is} value reflects a more uncompetitive type of inhibition. In other words, as the mode of inhibition becomes completely competitive, Kii $\rightarrow \infty$ and, therefore, K_{ii}/K_{is} approaches ∞.

Inhibitors showed a wide variation in potency, but, more importantly, also varied in degree of competiveness. In Table 1, inhibitors are ranked in order from least competitive to most competitive. 2,6-dichlorophenolindophenol (DCPIP) inhibited phthalazine oxidation with moderate micromolar potency and was the most uncompetitive of the compounds tested. Similar to the findings previously reported by Obach for raloxifene inhibition (Obach, 2004), the β-estradiol compounds of similar structure inhibited phthalazine oxidation predominantly through an uncompetitive mode. However, unlike raloxifene which was found to be exclusively uncompetitive, we observed a mixture of both competitive and uncompetitive inhibition. Menadione was also predominantly uncompetitive but both K_{is} and K_{ii} had a high degree of potency (nanomolar range). Domperidone inhibited mostly through a competitive mode, however, only with moderate micromolar potency. Chlorpromazine was mostly competitive with a K_{is} value in the nanomolar range. Of the compounds tested, only one compound, 6-chloroquinazolinone, was found to be exclusively competitive. This result was not surprising, as 6-chloroquinazolinone is a known substrate of AOX (Alfaro et al., 2009).

DMD Fast Forward. Published on September 22, 2011 as DOI: 10.1124/dmd.111.041806
This article has not been copyedited and formatted. The final version may differ from this version.

DISCUSSION

In a previous report, researchers determined that the selective estrogen receptor modulator raloxifene inhibited AOX through an exclusively uncompetitive mechanism (Obach, 2004). Generally, uncompetitive inhibitors are not considered to be significant candidates for drug interactions because the effect of such inhibitor is only realized at very high substrate concentrations (near saturating conditions). In vivo, the substrate concentrations are typically very low relative to K_m and, thus, an uncompetitive inhibitor would have very little effect on the rate of metabolism. However, since we have demonstrated that the mode of inhibition for these inhibitors is mixed (ie. containing both competitive and uncompetitive characteristics) the effect of the inhibitor is predicted to be significant even at substrate concentrations around K_m. This means at relatively low substrate concentrations, those typically found in vivo, the potential for drug-drug interactions is much greater than was previously suspected.

Predicting the magnitude of drug interactions in vivo using in vitro data is a difficult challenge. One coarse method for such a prediction uses the ratio of $[I]/K_i$ as a metric, where [I] is equal to the concentration of inhibitor in vivo. A value of 1 or greater is considered high risk for drug interactions, and a value between 1 and 0.1 is considered moderate risk. Any value less than 0.1 is considered a low risk of drug interactions (Tucker et al., 2001) and generally indicates further in vivo study is not required.

One of the key challenges when using this method to predict in vivo DDIs is selecting the most appropriate value for [I]. Previous attempts at defining the value for [I] that best approximates the concentration of inhibitor at the enzyme site have used peripheral vein concentration, hepatic portal vein concentration, average plasma concentration, maximum plasma concentration, hepatic input concentration, and hepatocyte concentration (Blanchard et al., 2004; Ito et al., 2004; Bachmann, 2006). For each of these values, both bound and unbound fractions can be used. To date, different choices for [I]

have had varying amounts of success, and there seems to be no clear consensus on which value for [I] is best (Bachmann, 2006). For the sake of simplicity, we chose to use maximum plasma concentration for [I] for this discussion. This value is easily accessible in the literature and provides a reasonable, albeit relatively less conservative, estimate for the concentration of inhibitor at the enzyme site.

Of the compounds tested, we looked at four for drug interaction potential using the above criteria: ethinyl estradiol, β-estradiol, clozapine, and chlorpromazine. These compounds were selected for discussion because of their clinical importance in man. In the case of ethinyl estradiol, clozapine, and chlorpromazine, these compounds are commonly administered drugs, and β-estradiol is an endogenous hormone.

Peak drug concentrations and $[I]/K_{is}$ values for the four clinically relevant inhibitors are shown in Table 2. Despite the K_{ii} values for some inhibitors being much more potent, K_{is} values were used in the calculation for all inhibitors in order to best approximate the potential drug interactions in vivo. For reasons discussed earlier, using a K_{ii} value for this calculation may lead to an erroneous prediction of potential drug interactions.

The results display an enormous range of $[I]/K_{is}$ values that are largely dependent on the concentration of drug found in vivo. Even in pregnant women, when β-estradiol levels are elevated, the concentration in vivo is very low relative to K_{is}. Similarly, ethinyl estradiol is typically taken at very low dosages in modern cocktails used as a contraceptive. As such, the plasma concentration never reaches anywhere near to the K_{is} value. The likelihood of drug interactions by the estrogenic compounds was found to be almost zero. However, the other two drugs we looked at are typically given to patients at much higher doses. Previous research has found that the plasma concentration of clozapine and chlorpromazine can reach as high as 1.7 μM and 0.5 μM respectively (Dahl and Strandjord, 1977; Brunton et al., 2006). For these drugs, the $[I]/K_{is}$ value are both between 0.1 and 1, indicating a moderate risk of drug interaction (Tucker et al., 2001). Further study would be required in vivo to determine whether a potential for drug interaction

exists. For example, co-administration of either chlorpromazine or clozapine with the sedative, zaleplon, (a known substrate for AOX1) could possibly lead to an undesired intensification of the sedative effect of the drug.

It should be noted, however, that the examples of potential "object" drugs that may be involved in drug interactions are few. The previously mentioned substrate Zaleplon, a sedative drug used primarily for the treatment of insomnia, is a nonbenzodiazepine hypnotic that is cleared primarily by AOX (Lake et al., 2002). Also, famciclovir, an antiviral prodrug used primarily to treat the herpes virus is activated by AOX to its active 6-oxo form, penciclovir (Clarke et al., 1995; Rashidi et al., 1997). Ziprasidone which is used to treat the symptoms of schizophrenia is metabolized by AOX (Beedham et al., 2003), as is the anti-cancer agent methotrexate (Jordan et al., 1999). These clinically used substrates are primarily but not exclusively metabolized by AOX with some portion of metabolism being through a pathway mediated by cytochrome P450 enzymes. As such, the likelihood of DDI due to inhibition of AOX is reduced. There is currently a lack of a highly selective substrate on the market that is metabolized via a pathway that is exclusively mediated by AOX. Therefore, a clinical study of DDIs caused by the inhibition of AOX may not currently be achievable. Still, despite relatively few substrates presently on the market, the importance of AOX as a drug clearing enzyme is predicted to increase markedly in the coming years primarily due to the growth in the nitrogen-containing heterocycles in drug candidates (Pryde et al., 2010). Perhaps a clinical substrate that is exclusively metabolized by AOX will be available in the near future.

The inhibition data described herein not only has implications on DDIs but also the inhibition mechanism. Mixed mode inhibition implies that the inhibitor has an affinity for both the "free" enzyme and the enzyme-substrate (E-S) complex. A lower K_{ii} value relative to K_{is} means that the inhibitor has a higher affinity for the E-S complex compared to the free enzyme. The traditional model for mixed inhibition involves one inhibitor binding site that is removed from the active site. This site may have its conformation altered by the presence or absence of substrate at the active site, such that the affinity for

inhibitor is different for free enzyme and E-S complex. This would explain the variation in degree of competitiveness for inhibitors found in the results of this study.

Researchers have previously found evidence of multiple egress sites for electron transfer (Rajagopalan and Handler, 1964). One possible explanation for inhibition is binding of the inhibitor to the electron transfer site, which prevents the electron transfer from reduced form of enzyme to molecular oxygen. This is supported by the fact that DCPIP, a known electron acceptor for AOX, was found to inhibit largely uncompetitively.

As shown in Table 1, the K_i values we measured were quite similar to the IC_{50} values determined by Obach et al (Obach et al., 2004). This demonstrates that an IC_{50} screening assay of HLC is quite effective for determining potent inhibitors of AOX in HLC from a large library of drugs. However, as was shown in cases of raloxifene and other estrogenic compounds, taking into account the IC_{50} value alone without any information regarding the mode of inhibition may lead to an over-prediction of drug interactions. We have shown that many inhibitors of AOX act primarily through an uncompetitive means such that any chance of drug interaction is slight. Therefore, due to the variation in competitiveness of various inhibitors, it appears that an effective strategy for determining whether or not the a potential for drug interactions in vitro exists would be to first screen compounds for IC_{50} and subsequently determine mode of inhibition by way of measuring K_i for the most potent inhibitors screened.

In conclusion, the inhibition of oxidation of phthalazine by human aldehyde oxidase was characterized for 8 different inhibitor compounds of largely varying structure. Of these 8, 7 were demonstrated to inhibit the enzyme though a mixed mode. Potential drug-drug interactions for potent pharmacologically relevant inhibitors were discussed. Future study in vivo is warranted to assess the prediction of a moderate risk of drug interactions with clozapine and chlorpromazine.

DMD Fast Forward. Published on September 22, 2011 as DOI: 10.1124/dmd.111.041806
This article has not been copyedited and formatted. The final version may differ from this version.

ACKNOWLEDGEMENTS

Special thanks to Upendra Dahal for his helpful discussion concerning mass spectrometry assays.

AUTHORSHIP CONTRIBUTIONS

Participated in research design: Barr, Jones
Conducted experiments: Barr
Contributed new reagents or analytic tools: N/A
Performed data analysis: Barr
Wrote or contributed to the writing of the manuscript: Barr, Jones

REFERENCES

Alfaro JF, Joswig-Jones CA, Ouyang W, Nichols J, Crouch GJ, and Jones JP (2009) Purification and Mechanism of Human Aldehyde Oxidase Expressed in Escherichia coli. *Drug Metab Dispos* **37:**2393-2398.

Bachmann KA (2006) Inhibition constants, inhibitor concentrations and the prediction of inhibitory drug drug interactions: pitfalls, progress and promise. *Curr Drug Metab* **7:**1-14.

Beedham C, Miceli JJ, and Obach RS (2003) Ziprasidone metabolism, aldehyde oxidase, and clinical implications. *J Clin Psychopharmacol* **23:**229-232.

Bibi Z (2008) Role of cytochrome P450 in drug interactions. *Nutr Metab* **5:**27.

Blanchard N, Richert L, Coassolo P, and Lave T (2004) Qualitative and quantitative assessment of drug-drug interaction potential in man, based on Ki, IC50 and inhibitor concentration. *Curr Drug Metab* **5:**147-156.

Brandaenge S and Lindblom L (1979) The enzyme "aldehyde oxidase" is an iminium oxidase. Reaction with nicotine delta 1'(5') iminium ion. *Biochem Biophys Res Commun* **91:**991.

Brunton LL, Gilman A, and Goodman LS (2006) *Goodman & Gilman's the pharmacological basis of therapeutics*. McGraw-Hill, New York [u.a.].

Chiba M, Jin L, Neway W, Vacca JP, Tata JR, Chapman K, and Lin JH (2001) P450 interaction with HIV protease inhibitors: relationship between metabolic stability, inhibitory potency, and P450 binding spectra. *Drug Metab Dispos* **29:**1-3.

Clarke SE, Harrell AW, and Chenery RJ (1995) Role of aldehyde oxidase in the in vitro conversion of famciclovir to penciclovir in human liver. *Drug Metab Dispos* **23:**251.

Cook PB and Cleland WW (2007) *Enzyme Kinetics and Mechanism*. Garland Science, New York.

Dahl SG and Strandjord RE (1977) Pharmacokinetics of chlorpromazine after single and chronic dosage. *Clin Pharmacol Ther* **21:**437.

Garattini E and Terao M (2011) Increasing recognition of the importance of aldehyde oxidase in drug development and discovery. *Drug Metab Rev*.

Ito K, Brown HS, and Houston JB (2004) Database analyses for the prediction of in vivo drug-drug interactions from in vitro data. *Br J Clin Pharmacol* **57:**473-486.

Jordan CG, Rashidi MR, Laljee H, Clarke SE, Brown JE, and Beedham C (1999) Aldehyde oxidase-catalysed oxidation of methotrexate in the liver of guinea-pig, rabbit and man. *J Pharm Pharmacol* **51:**411-418.

Lake B, Ball SE, Kao J, Renwick A, Price RJ, and Scatina JA (2002) Metabolism of zaleplon by human liver: evidence for involvement of aldehyde oxidase. *Xenobiotica* **32:**835.

Obach RS (2004) Potent Inhibition of Human Liver Aldehyde Oxidase By Raloxifene. *Drug Metab Dispos* **32:**89-97.

Obach RS, Huynh P, Allen MC, and Beedham C (2004) Human Liver Aldehyde Oxidase: Inhibition by 239 Drugs. *J Clin Pharmacol* **44:**7-19.

Ortiz de Montellano PR (2005) *Cytochrome P450: Structure, Mechanism, and Biochemistry, 3rd ed*. Plenum, New York.

Panoutsopoulos G and Beedham C (2004) Enzymatic oxidation of phthalazine with guinea pig liver aldehyde oxidase and liver slices: inhibition by isovanillin. *Acta Biochimica Polonica* **51:**943.

Peng CC, Pearson JT, Rock DA, Joswig-Jones CA, and Jones JP (2010) The effects of type II binding on metabolic stability and binding affinity in cytochrome P450 CYP3A4. *Arch Biochem Biophys* **497:**68-81.

Piwowarska J, Radowicki S, and Pachecka J (2009) Simultaneous determination of eight estrogens and their metabolites in serum using liquid chromatography with electrochemical detection. *Talanta* **81:**275-280.

Pryde DC, Dalvie D, Hu Q, Jones P, Obach RS, and Tran T-D (2010) Aldehyde Oxidase: An Enzyme of Emerging Importance in Drug Discovery. *J Med Chem* **53:**8441-8460.

Rajagopalan KV and Handler P (1964) Hepatic Aldehyde Oxidase. *J Biol Chem* **239:**2027-2035.

Rashidi M, Smith JA, Clarke SE, and Beedham C (1997) In vitro oxidation of famciclovir and 6-deoxypenciclovir by aldehyde oxidase from human, guinea pig, rabbit, and rat liver. *Drug Metab Dispos* **25:**805.

Tucker GT, Houston JB, and Huang S-M (2001) Optimizing drug development: strategies to assess drug metabolism/transporter interaction potential-toward a consensus. *Pharm Res* **18:**1071.

Westhoff CL, Torgal AH, Mayeda ER, Pike MC, and Stanczyk FZ (2010) Pharmacokinetics of a combined oral contraceptive in obese and normal-weight women. *Contraception* **81:**474-480.

Whittlesea CMC and Gorrod W (1993) The enzymology of the in-vitro oxidation of prolintane to oxoprolintane. *J Clin Pharm Ther* **18:**357.

FOOTNOTES

This work was supported by the National Institutes of Health National Institute of General Medical Sciences [GM84546]

LEGENDS FOR FIGURES

Figure 1- Structures of human liver aldehyde oxidase inhibitors

Figure 2- Oxidation reaction of phthalazine to 1-phthalazinone. Structure of IS used for mass spectrometry assay provided on right.

Figure 3- Saturation kinetics plot for oxidation of phthalazine. Each point represents an average ± standard error a minimum of 8 different experiments.

Figure 4- Lineweaver-burk plots and slope/intercept replots of phthalazine oxidation inhibition by 8 different inhibitors: A) DCPIP B) estradiol C) menadione D) ethinyl estradiol E) domperidone F)Chlorpromazine G) Clozapine H)6-chloroquinazolinone (6-CQ) . Each point reflects the average of triplicate determinations.

DMD Fast Forward. Published on September 22, 2011 as DOI: 10.1124/dmd.111.041806
This article has not been copyedited and formatted. The final version may differ from this version.

Table 1. K_{is} and K_{ii} values for AOX. Each value reflects an average ± standard error for two determinations.

Inhibitor	K_{is} (μM)	K_{ii} (μM)	K_{ii}/K_{is}	IC_{50}[a]
DCPIP	19 ± 1.8	2.4 ± 0.18	0.13	ND
β-Estradiol	0.9 ± 0	0.13 ± 0	0.14	0.29 ± 0.07
Menadione	0.75 ± 0.18	0.12 ± 0	0.16	0.20 ± 0.04
Ethinyl estradiol	1.1 ± 0.32	0.23 ± 0.011	0.21	0.57 ± 0.15
Domperidone	5.3 ± 2.6	14 ± 2.8	2.6	3.0 ± 1.4
Chlorpromazine	0.62 ± 0.23	3.3 ± 0.53	5.3	0.57 ± 0.15
Clozapine	3.9 ± 0.35	60 ± 1.8	15	4.4 ± 1.8
6-Chloroquinazolinone	5.4 ± 0.92	--	--	ND

[a]Measured in previous study by Obach and coworkers (Obach et al., 2004).

DMD Fast Forward. Published on September 22, 2011 as DOI: 10.1124/dmd.111.041806
This article has not been copyedited and formatted. The final version may differ from this version.

Table 2. Human peak plasma concentrations ([I]) and K_{is} values for AOX inhibitors. [I]/K_{is} represents an estimate of likelihood of drug interactions in vivo.

Inhibitor	**[I]** *(nM)*	**K_{is}** *(nM)*	**[I]/K_{is}**
Ethinyl estradiol	0.44[a]	1100	0.0004
β-Estradiol	12[b]	900	0.01
Clozapine	1700[c]	3900	0.4
Chlorpromazine	470[d]	620	0.8

[a] for normal women given a 30 μg dose (Westhoff et al., 2010)

[b] in pregnant women (Piwowarska et al., 2009)

[c] for patients given 150mg dose twice a day for 7 days (Brunton et al., 2006)

[d] for patients given 100mg a day for 30 days (Dahl and Strandjord, 1977)

Figure 1

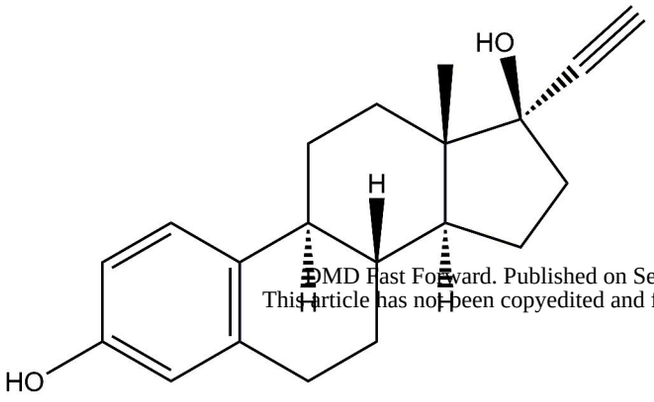

ethinyl estradiol

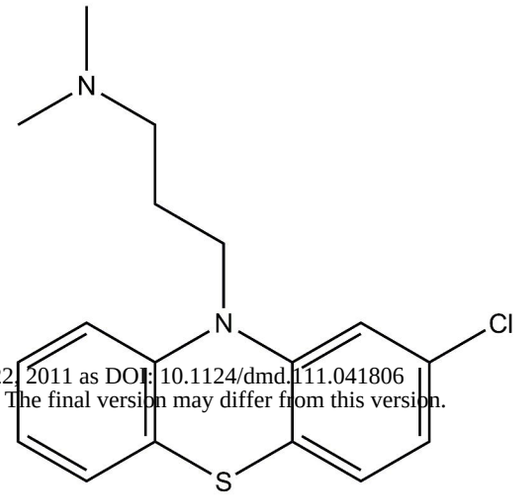

chlorpromazine

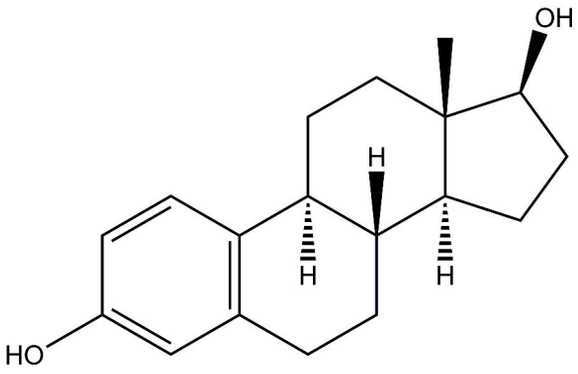

estradiol

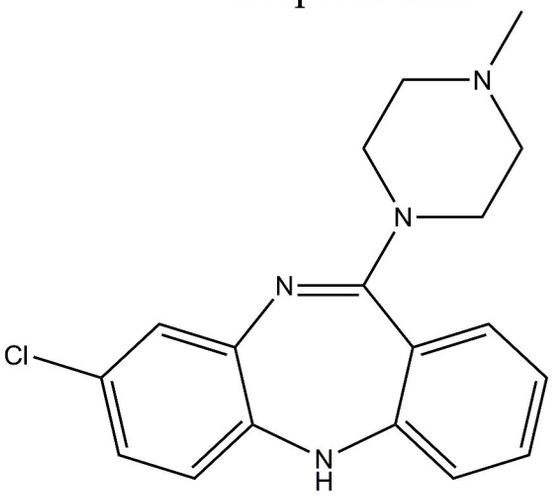

clozapine

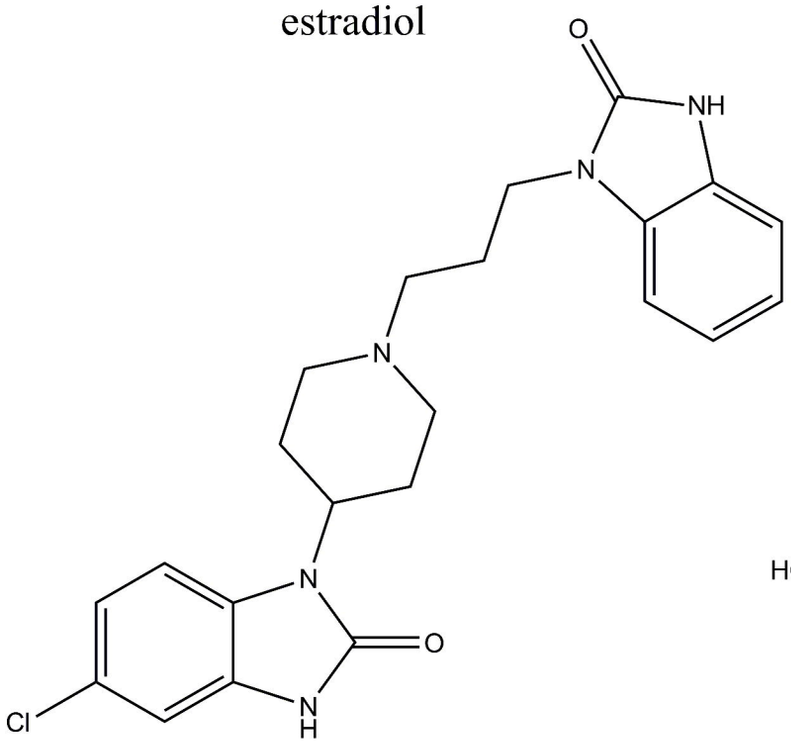

domperidone

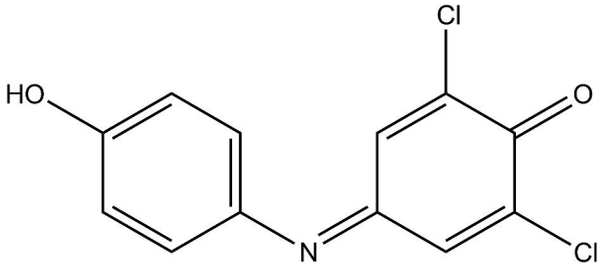

2,6-dichlorophenolindophenol

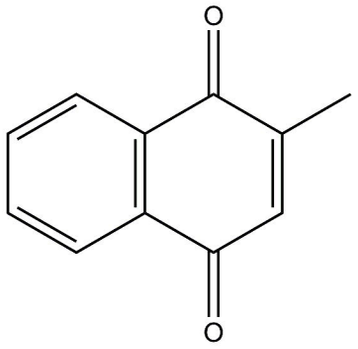

menadione

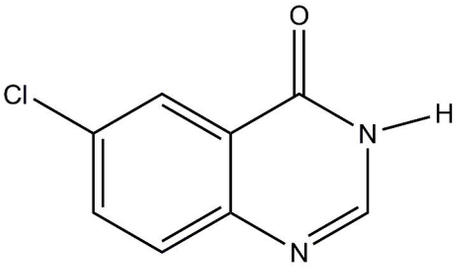

6-chloroquinazolinone

Figure 2

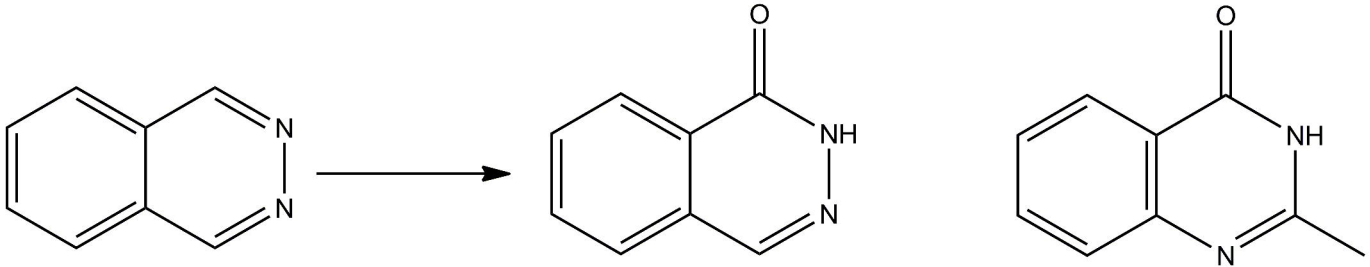

phthalazine

1-phthalazinone

2-methyl-4(3H)-quinazolinone (IS)

Figure 3

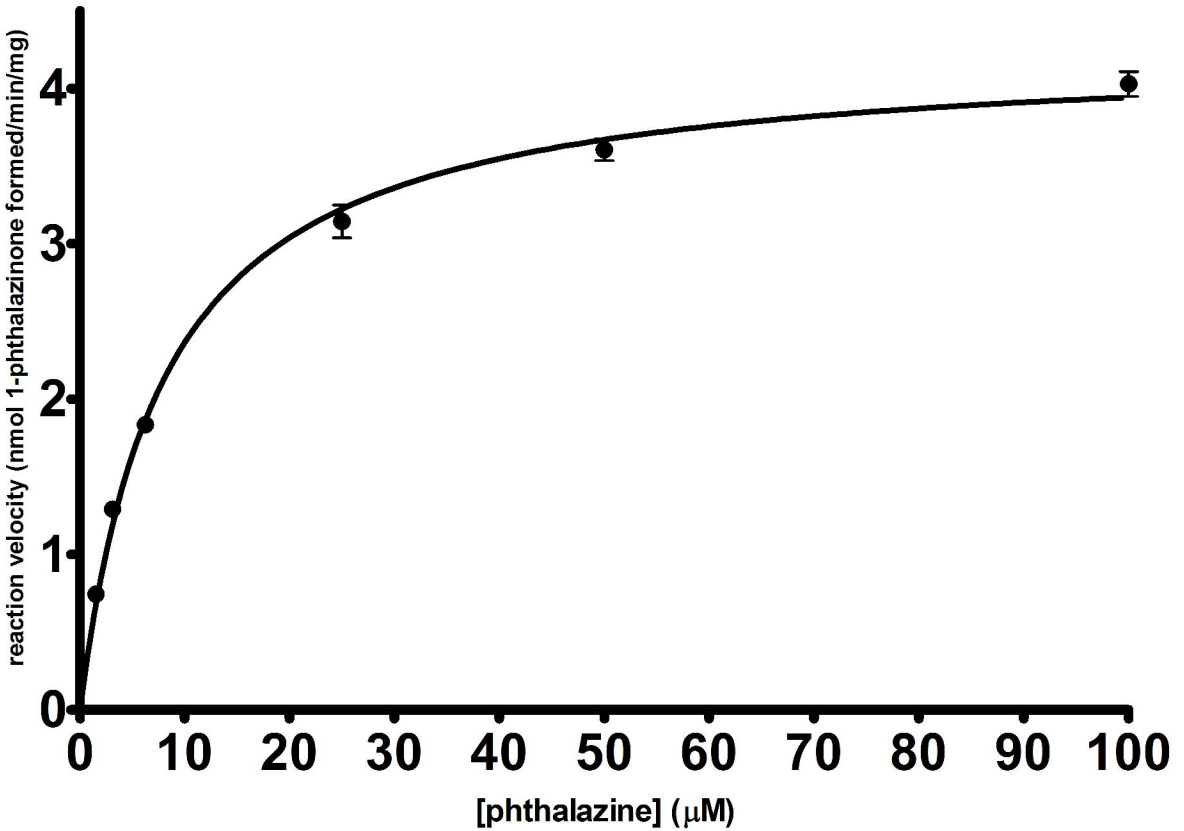
reaction velocity (nmol 1-phthalazinone formed/min/mg)
0
1
2
3
4
0
10
20
30
40
50
60
70
80
90
100
[phthalazine] (μM)

DMD Fast Forward. Published on September 22, 2011 as DOI: 10.1124/dmd.111.041806
This article has not been copyedited and formatted. The final version may differ from this version.

Figure 4